Evolutionary Ecology Research, 2002, **4**: 189–217

Ontogenetic niche shifts and evolutionary branching in size-structured populations

David Claessen[1]* and Ulf Dieckmann[2]

[1]*Institute for Biodiversity and Ecosystem Dynamics, Section of Population Biology, University of Amsterdam, PO Box 94084, 1090 GB Amsterdam, The Netherlands and* [2]*Adaptive Dynamics Network, International Institute for Applied Systems Analysis, A-2361 Laxenburg, Austria*

ABSTRACT

There are many examples of size-structured populations where individuals sequentially exploit several niches in the course of their life history. Efficient exploitation of such ontogenetic niches generally requires specific morphological adaptations. Here, we study the evolutionary implications of the combination of an ontogenetic niche shift and environmental feedback. We present a mechanistic, size-structured model in which we assume that predators exploit one niche when they are small and a second niche when they are big. The niche shift is assumed to be irreversible and determined genetically. Environmental feedback arises from the impact that predation has on the density of the prey populations. Our results show that, initially, the environmental feedback drives evolution towards a generalist strategy that exploits both niches equally. Subsequently, it depends on the size-scaling of the foraging rates on the two prey types whether the generalist is a continuously stable strategy or an evolutionary branching point. In the latter case, divergent selection results in a resource dimorphism, with two specialist subpopulations. We formulate the conditions for evolutionary branching in terms of parameters of the size-dependent functional response. We discuss our results in the context of observed resource polymorphisms and adaptive speciation in freshwater fish species.

Keywords: Arctic char, bluegill, cichlids, evolution, feedback, ontogenetic niche shift, perch, population dynamics, resource polymorphism, roach, size structure.

INTRODUCTION

In size-structured populations, it is common for individuals to exploit several niches sequentially in the course of their life history (Werner and Gilliam, 1984). The change during life history from one niche to another is referred to as an ontogenetic niche shift. The shift can be abrupt, such as that associated with metamorphosis in animals like tadpoles and insects, or gradual, such as the switch from planktivory to benthivory in many freshwater fish species (Werner, 1988).

* Address all correspondence to David Claessen, IACR-Rothamsted, Biomathematics Unit, Harpenden, Herts AL5 2JQ, UK. e-mail: david.claessen@bbsrc.ac.uk

Ontogenetic niche shifts have been interpreted as adaptations to the different energetic requirements and physiological limitations of individuals of different sizes. The profitability of a given prey type generally changes with consumer body size because body functions such as capture rate, handling time, digestion capacity and metabolic rate depend on body size. For example, using optimal foraging theory, both the inclusion of larger prey types in the diet of larger Eurasian perch (*Perca fluviatilis*) individuals, and the ontogenetic switch from the pelagic to the benthic habitat, have been attributed to size-dependent capture rates and handling times (Persson and Greenberg, 1990). Determining the optimal size at which an individual is predicted to shift from one niche to the next, and how the optimum depends on the interactions between competing species, have been at the focus of ecological research during the last two decades (Mittelbach, 1981; Werner and Gilliam, 1984; Persson and Greenberg, 1990; Leonardsson, 1991). Research has concentrated on approaches based on optimization at the individual level, assuming a given state of the environment in terms of food availability and mortality risks. An important result of this research is Gilliam's μ/g rule, which states that (for juveniles) the optimal strategy is to shift between niches in such a way that the ratio of mortality over individual growth rate is minimized at each size (Werner and Gilliam, 1984).

Individual-level optimization techniques do not take into account population-level consequences of the switch size. In particular, the size at which the niche shift occurs affects the harvesting pressures on the different prey types and hence their equilibrium densities. In an evolutionary context, this ecological feedback between the strategies of individuals and their environment has to be taken into account. On the one hand, the optimal strategy depends on the densities of the resources available in the different niches. On the other hand, these resource densities change with the ontogenetic strategies and resultant harvesting rates of individuals within the consumer population. A framework for the study of evolution in such an ecological context is the theory of adaptive dynamics (Metz *et al.*, 1992, 1996a; Dieckmann and Law, 1996; Dieckmann and Doebeli, 1999; Doebeli and Dieckmann, 2000). In this framework, the course and outcome of evolution are analysed by deriving the fitness of mutants from a model of the ecological interactions between individuals and their environment. An important result from adaptive dynamics theory is that, if fitness is determined by frequency- and/or density-dependent ecological interactions, evolution by small mutational steps can easily give rise to evolutionary branching. However, although most species are size-structured (Werner and Gilliam, 1984; Persson, 1987), the adaptive dynamics of size-structured populations have received little attention so far. Although there have been several studies of adaptive dynamics in age- or stage-structured populations (e.g. Heino *et al.*, 1997; Diekmann *et al.*, 1999), only one of these explicitly accounted for the effects of the environment on individual growth and on population size structure (Ylikarjula *et al.*, 1999). One motivation for the research reported here, therefore, is to determine similarities and differences between evolution in structured and unstructured populations subject to frequency- and density-dependent selection. We can even ask whether population size structure has the potential to drive processes of evolutionary branching that would be absent, and thus overlooked, in models lacking population structure.

In this paper, we examine a simple size-structured population model that includes a single ontogenetic niche shift. The ecological feedback is incorporated by explicitly taking resource dynamics into account. We assume that individuals exploit one prey type when they are small and another prey type when they are big. The ontogenetic niche shift is

thought to represent a morphological trade-off: if efficient exploitation of either prey type requires specific adaptations, shifting to the second prey type results in a reduced efficiency on the first prey type. The size at which individuals shift from the first to the second niche is assumed to be determined genetically and is the evolutionary trait in our analysis. The shift is assumed to be gradual; we investigate how evolutionary outcomes are influenced by the width of the size interval with a mixed diet.

We focus on two specific questions. First, what is the effect of the ecological feedback loop through the environment on the evolution of the ontogenetic niche shift? The size at which individuals shift to the second niche affects the predation rate on both prey types and hence their abundances. The relation between strategy and prey abundance is likely to be important for the evolution of the ontogenetic niche shift. Second, what is the effect of the scaling with body size of search and handling rates for the two prey types? The profitability of prey types for an individual of a certain size depends on how these vital rates vary with body size. Data exist for several species on how capture rates and handling times depend on body size. Thus, if different evolutionary scenarios can be attributed to differences in these scaling relations, the results reported here may help to compare different species and to assess their evolutionary histories in terms of the ecological conditions they experience.

THE MODEL

As the basis for our analysis, we consider a physiologically structured population model of a continuously reproducing, size-structured population. We assume that the structured population feeds on two dynamic prey populations. Our model extends the Kooijman-Metz model (Kooijman and Metz, 1984; de Roos *et al.*, 1992; de Roos, 1997) in two directions: first, by introducing a second prey population and, second, by the generalization of the allometric functions for search rate and handling time that determine the functional response.

Individuals are characterized by two so-called *i*-state variables (Metz and Diekmann, 1986): their current length, denoted by x, and the length around which they switch from the first to the second prey type, denoted by u (Table 1). Individuals are assumed to be born with length x_b; subsequently, their length changes continuously over time as a function of food intake and metabolic costs. The switch size u is constant throughout an individual's life but, in our evolutionary analysis, may change from parent to offspring by mutation. In our analysis of the population dynamic equilibrium, we assume monomorphic populations, in which all individuals have the same trait value u. The per capita mortality rate, denoted μ, is assumed to be constant and size-independent. Possible consequences of relaxing this assumption are addressed in the Discussion, under the heading 'Assumptions revisited'.

Feeding

Individuals start their lives feeding on prey 1 but shift (gradually or stepwise) to prey 2 as they grow. We assume a complementary relation between foraging efficiencies on the two prey types, which is thought to be caused by a genetically determined morphological change during ontogeny. Figure 1 shows two sigmoidal curves as a simple model of such an ontogenetic niche shift. Immediately after birth, individuals have essentially full efficiency on prey 1 but are very inefficient on prey 2. At the switch size $x = u$, individuals have equal

Table 1. Symbols used in model definition for state variables[a] and constant parameters

Symbol	Value	Unit	Interpretation
Variables[a]			
x		cm	*i*-state: length
u		cm	*i*-state: length at ontogenetic niche shift
$n(x, u)$		—[b]	*p*-state: population size-distribution
F_1, F_2		m^{-3}	*E*-state: population density of prey type 1, 2
Constants			
x_b	0.5	cm	length at birth
λ	0.01	$\mathrm{g \cdot cm^{-3}}$	length–weight constant
a_1, a_2	(1–10)	$\mathrm{m^3 \cdot day^{-1} \cdot cm^{-q}}$	maximum attack rate scaling constants (prey types 1, 2)
q_1, q_2	(1–3)	—	maximum attack rate scaling exponent
k	(1–1000)	—	abruptness of ontogenetic niche shift
h_1, h_2	(10–100)	$\mathrm{day \cdot g^{-1} \cdot cm^{-p}}$	handling time constant, prey type 1
p	(1–3)	—	handling time scaling exponent
ε	0.65	—	intake coefficient
ρ	2.5×10^{-4}	$\mathrm{g \cdot day^{-1} \cdot mm^{-3}}$	metabolic rate constant
κ	0.7	—	allocation coefficient
σ	1.25×10^{-3}	—	energy for one offspring
μ	0.1	$\mathrm{day^{-1}}$	background mortality rate
r_1, r_2	(0.1)	$\mathrm{day^{-1}}$	prey 1, 2 population growth rate
K_1, K_2	(0.1)	$\mathrm{g \cdot m^{-3}}$	prey 1, 2 carrying capacity

[a] To avoid excessive notation, we dropped the time argument.
[b] The dimension of n is density ($\mathrm{m^{-3}}$) after integration over *i*-state space; that is, $\int n(x, u)\, \mathrm{d}u\, \mathrm{d}x$.
Note: For the parameters that are varied between runs of the model, the range of values or the default value is given in parentheses.

efficiency on both prey types. Larger individuals become increasingly more specialized on prey type 2.

The ontogenetic niche shift is incorporated into the model by assuming that the attack rate on each prey type is the product of an allometric term that increases with body length, and a 'shift' term that is sigmoidal in body length and that depends on the switch size u. Using a logistic sigmoidal function for the shift term (Fig. 1), the two attack rate functions become:

$$A_1(x,u) = a_1 x^{q_1} \frac{1}{1 + \mathrm{e}^{k(x-u)}} \tag{1}$$

$$A_2(x,u) = a_2 x^{q_2} \left(1 - \frac{1}{1 + \mathrm{e}^{k(x-u)}} \right) \tag{2}$$

where a_1 and a_2 are allometric constants and q_1 and q_2 are allometric exponents. The parameter k tunes the abruptness of the switch; $k = \infty$ corresponds to a discrete step from niche 1 to niche 2 at size $x = u$, whereas a small value of k (e.g. $k = 20$) describes a more gradual shift. In the latter case, there is a considerable size interval over which individuals have a mixed diet.

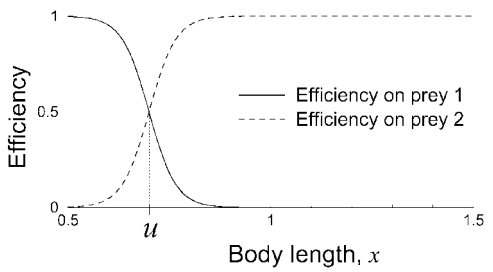

Fig. 1. A simple model of an ontogenetic niche shift. Size $x = u$ is referred to as the 'switch size' and is assumed to be a genetic trait ($u = 0.7$, $k = 30$).

If we let the switch size u increase to infinity, the attack rate on prey type 1 approaches the allometric term for all lengths. Similarly, if we let the switch size decrease to minus infinity, the attack rate on prey type 2 approaches the allometric term. In the rest of this article, we frequently make use of these two limits, denoted $\hat{A}_i(x)$:

$$\hat{A}_1(x) = \lim_{u \uparrow \infty} A_1(x,u) = a_1 x^{q_1} \tag{3}$$

$$\hat{A}_2(x) = \lim_{u \downarrow -\infty} A_2(x,u) = a_2 x^{q_2} \tag{4}$$

Since the functions $\hat{A}_i(x)$ correspond to the highest possible attack rates on prey type i at body length x, we refer to them as the *possible* attack rates. Accordingly, the functions $A_i(x, u)$ (equations 1 and 2) are referred to as the *actual* attack rates.

The digestive capacity is assumed to increase with body size, which results in handling times per unit of prey weight that decrease with body size, $H_i(x)$:

$$H_1(x) = h_1 x^{-p} \tag{5}$$

$$H_2(x) = h_2 x^{-p} \tag{6}$$

While we assume that the same allometric exponent $-p$ applies to both prey types, these types may differ in digestibility and the allometric constants h_1 and h_2 may therefore differ. We assume a Holling type II functional response for two prey species:

$$f(x,u,F_1,F_2) = \frac{A_1(x,u)F_1 + A_2(x,u)F_2}{1 + A_1(x,u)H_1(x)F_1 + A_2(x,u)H_2(x)F_2} \tag{7}$$

where F_1 and F_2 denote the densities of the two prey populations, respectively.

Extrapolating the terminology that we use for attack rates, we refer to the function $f(x,u,F_1,F_2)$ as the 'actual' intake rate. In the analysis below, we use the term 'possible' intake rate to refer to the intake rate of an individual that focuses entirely on one of the two niches. It is given by

$$\hat{f}_i(x,F_i) = \frac{\hat{A}_i(x)F_i}{1 + \hat{A}_i(x)H_i(x)F_i} \tag{8}$$

with $i = 1$ for the first niche and $i = 2$ for the second one, and where $\hat{A}_i(x)$ is the possible attack rate on prey type i. Note that $f_1(x,F_1)$ and $f_2(x,F_2)$ are obtained by taking the limit of $f(x,u,F_1,F_2)$ as u approaches ∞ and $-\infty$, respectively.

Reproduction and growth

The energy intake rate is assumed to equal the functional response multiplied by a conversion efficiency ε. A fixed fraction $1 - \kappa$ of the energy intake rate is channelled to reproduction. Denoting the energy needed for a single offspring by σ, the per capita birth rate equals

$$b(x, u, F_1, F_2) = \frac{\varepsilon(1-\kappa)}{\sigma} f(x, u, F_1, F_2) \tag{9}$$

To restrict the complexity of our model, we assume that individuals are born mature and that reproduction is clonal. The fraction κ of the energy intake rate is used to cover metabolism first and the remainder is used for somatic growth. Assuming that the metabolic rate scales with body volume (proportional to x^3), the growth rate in body mass becomes:

$$G_m(x, u, F_1, F_2) = \varepsilon\kappa f(x, u, F_1, F_2) - \rho x^3$$

where ρ is the metabolic cost per unit of volume. Assuming a weight–length relation of the form $W(x) = \lambda x^3$, and using $\mathrm{d}x/\mathrm{d}t = (\mathrm{d}w/\mathrm{d}t)(\mathrm{d}x/\mathrm{d}w)$, we can write the rate of growth in length as:

$$g(x, u, F_1, F_2) = \frac{1}{3\lambda x^2}(\varepsilon\kappa f(x, u, F_1, F_2) - \rho x^3) \tag{10}$$

The length at which the growth rate becomes zero is referred to as x_{max}. Individuals with a size beyond x_{max} have a negative growth rate (but a positive birth rate). Since in the analysis below we assume population dynamic equilibrium, we ensure that no individual grows beyond the maximum size. Note that in the special case with $p = q_1 = q_2 = 2$ the function g becomes linear in x, yielding the classic von Bertalanffy growth model (von Bertalanffy, 1957).

Prey dynamics

The population size distribution is denoted by $n(x, u)$. For the analyses of the deterministic model below, we assume that the (resident) population is monomorphic in u. Therefore, we do not have to integrate over switch sizes u but only over sizes x to obtain the total population density,

$$N_{tot}(u) = \int_{x_b}^{x_{max}} n(x, u)\, \mathrm{d}x \tag{11}$$

We assume that the two prey populations grow according to semi-chemostat dynamics and that they do not interact with each other directly. The dynamics of the prey populations can then be described by:

$$\frac{\mathrm{d}F_1}{\mathrm{d}t} = r_1(K_1 - F_1) - \int_{x_b}^{x_{max}} \frac{A_1(x, u)\, F_1}{1 + A_1(x,u)H_1(x)F_1 + A_2(x,u)H_2(x)F_2} n(x,u)\, \mathrm{d}x \tag{12}$$

$$\frac{\mathrm{d}F_2}{\mathrm{d}t} = r_2(K_2 - F_2) - \int_{x_b}^{x_{max}} \frac{A_2(x,u)F_2}{1 + A_1(x,u)H_1(x)F_1 + A_2(x,u)H_2(x)F_2} n(x,u)\, \mathrm{d}x \tag{13}$$

where r_1, r_2, K_1 and K_2 are the maximum growth rates and maximum densities of the two prey populations, respectively. The integral term in each equation represents the predation pressure imposed by the predator population.

The PDE formulation of the model is given in Table 2 and the individual level model is summarized in Table 3.

Parameterization

Since we intend to study the effect of the size-scaling of the functional response on the evolution of the ontogenetic niche shift, the parameters a_1, a_2, h_1, h_2, p, q_1 and q_2 are not fixed. Depending on whether handling time and search rate are determined by processes related to body length, surface or volume, the allometric exponents p, q_1 and q_2 are close to 1, 2 or 3, respectively. The remaining, fixed parameters are based on the parameterization of a more detailed model of perch (Claessen *et al.*, 2000).

ECOLOGICAL DYNAMICS

Before we can study evolution of the ontogenetic niche shift, we have to assess the effect of the ontogenetic niche shift on the ecological dynamics. Our model (Table 2) is not analytically solvable. Instead, we study its dynamics through a numerical method for the integration of physiologically structured population models, called the Escalator Boxcar Train (de Roos *et al.*, 1992; de Roos, 1997). When restricting attention to a single prey type (which is equivalent to assuming $u \gg x_{\max}$) and to the special case $p = q_1 = 2$, our model reduces to the Kooijman-Metz model, of which the population dynamics are well documented in the literature (e.g. de Roos *et al.*, 1992; de Roos, 1997). Numerical studies of the equilibrium behaviour of this simplified model show that the population dynamics always converge to a stable equilibrium, which can be attributed to the absence of a juvenile delay and to the semi-chemostat (rather than, for example, logistic) prey dynamics (cf. de Roos, 1988; de Roos *et al.*, 1990). Simulations show that, also for the general functional

Table 2. The model: specification of dynamics[a]

PDE	$\dfrac{\partial n}{\partial t} + \dfrac{\partial gn}{\partial x} = -\mu n(x,u)$
Boundary condition	$g(x_b, u, F_1, F_2)n(x_b, u) = \int_{x_b}^{x_{\max}} b(x, u, F_1, F_2)n(x,u)\,\mathrm{d}x$
Prey dynamics	$\dfrac{\mathrm{d}F_1}{\mathrm{d}t} = r_1(K_1 - F_1) - \int_{x_b}^{x_{\max}} \dfrac{A_1(x,u)F_1}{1 + A_1(x,u)H_1(x)F_1 + A_2(x,u)H_2(x)F_2} n(x,u)\,\mathrm{d}x$
	$\dfrac{\mathrm{d}F_2}{\mathrm{d}t} = r_2(K_2 - F_2) - \int_{x_b}^{x_{\max}} \dfrac{A_2(x,u)F_2}{1 + A_1(x,u)H_1(x)F_1 + A_2(x,u)H_2(x)F_2} n(x,u)\,\mathrm{d}x$

[a] The time argument has been left out from all variables and functions.
Note: The functions defining the birth rate (b), growth rate (g), attack rates (A_1, A_2) and handling times (H_1, H_2) are listed in Table 3, parameters in Table 1. PDE = partial differential equation.

Table 3. The model: individual level functions

Attack rate on prey 1	$A_1(x,u) = a_1 x^{q_1} \dfrac{1}{1+\mathrm{e}^{k(x-u)}}$
Attack rate on prey 2	$A_2(x,u) = a_2 x^{q_2}\left(1 - \dfrac{1}{1+\mathrm{e}^{k(x-u)}}\right)$
Handling time, prey 1	$H_1(x) = h_1 x^{-p}$
Handling time, prey 2	$H_2(x) = h_2 x^{-p}$
Functional response	$f(x,u,F_1,F_2) = \dfrac{A_1(x,u)F_1 + A_2(x,u)F_2}{1 + A_1(x,u)H_1(x)F_1 + A_2(x,u)H_2(x)F_2}$
Maintenance requirements	$M(x) = \rho x^3$
Growth rate in length	$g(x,u,F_1,F_2) = \dfrac{1}{3\lambda x^2}\left(\kappa\varepsilon f(x,u,F_1,F_2) - \rho x^3\right)$
Birth rate	$b(x,u,F_1,F_2) = \dfrac{\varepsilon(1-\kappa)}{\sigma} f(x,u,F_1,F_2)$

response (with values of p, q_1 and q_2 between 1 and 3), the equilibrium is stable for all investigated parameter combinations.

It is possible to choose parameter values (e.g. small K_i or high h_i) for which the predator population cannot persist on either prey 1 or prey 2 alone. In the results presented below, we use parameter values that allow for persistence on either prey type separately.

Ontogenetic niche shift and prey densities

We now examine the ecological effect of the size at the ontogenetic niche shift on the equilibrium state of a monomorphic size-structured population and the two prey populations. Each specific choice of u and the parameters results in a stable size distribution $n(x,u)$ and equilibrium prey densities F_1 and F_2. The effect of the switch size u on the prey densities F_1 and F_2, on the total predator population density $N_{\mathrm{tot}}(u)$ and on the the maximum length in the predator population $x_{\max}$ is shown in Fig. 2 for two different parameter combinations.

Three conclusions can readily be drawn from Fig. 2. First, prey density F_1 or F_2 is low if most of the predator population consumes prey 1 or prey 2, respectively. Second, the total number of predators, $N_{\mathrm{tot}}(u)$, reaches a maximum for an intermediate switch size u (i.e. when predators exploit both prey). Third, the maximum length in the predator population correlates strongly with the density of the second prey provided that individuals reach the size at which the ontogenetic niche occurs (i.e. $x_{\max} > u$).

With very low or very high u, the system reduces to a one-consumer, one-resource system. If the switch size is very large ($u > x_{\max}$; for example, $u > 2.5$ in Fig. 2), individuals never reach a size large enough to start exploiting the second prey. The second prey population is hence at the carrying capacity K_2, whereas the first prey is heavily exploited. Similarly, for a very small switch size ($u < x_{\mathrm{b}}$; for example, $u = 0$ in Fig. 2), even newborns have a low efficiency on prey type 1. In this case, prey 1 is near its carrying capacity K_1 and prey 1 is depleted. The two extreme strategies $u > x_{\max}$ and $u < x_{\mathrm{b}}$, therefore, characterize specialists

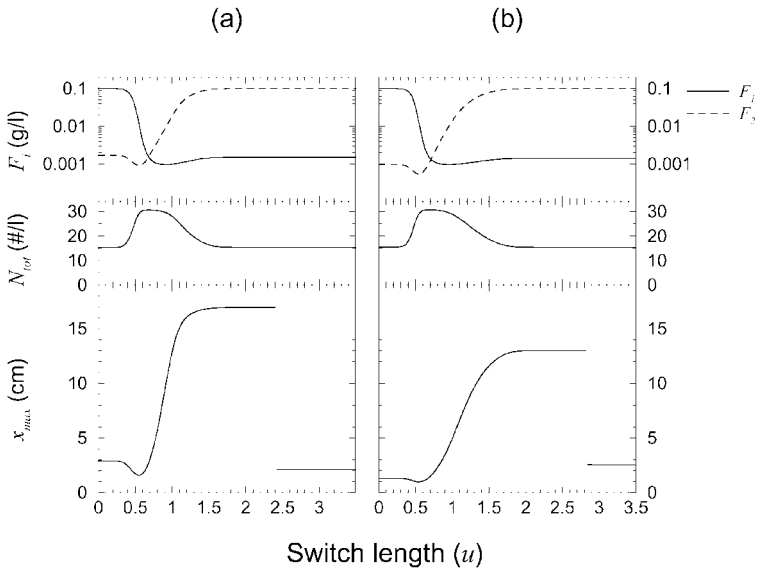

Fig. 2. The ecological equilibrium of a monomorphic population, as a function of the length at ontogenetic niche shift (u), characterized by prey densities (upper panels), total predator density (middle panels) and maximum length in predator population (lower panels). (a) Parameters: $q_1 = 1.8$, $q_2 = 2.1$, $h_1 = h_2 = 100$. (b) Parameters: $q_1 = 2$, $q_2 = 1$, $h_1 = h_2 = 10$. Other parameters (in both cases), $p = 2$, $k = 30$ and as in Table 1.

on prey 1 and prey 2, respectively. Although at first sight a strategy $u < x_b$ appears to be biologically meaningless, it can be interpreted as a population that has lost the ability to exploit a primary resource which its ancestors used to exploit in early life stages. This evolutionary scenario turns up in the results (see pp. 208–210).

A striking result evident from Fig. 2 is the discontinuous change in maximum length at high values of u. For u beyond the discontinuity, growth in the first niche is insufficient to reach the ontogenetic niche shift, such that the maximum length is determined only by the prey density in the first niche. As soon as the switch size is reachable in the first niche, the maximum size is determined by the prey density in the second niche. Just to the left of the discontinuity, only a few individuals live long enough to enter the second niche, and the impact of these individuals on the second prey is negligible ($F_2 \approx K_2$). These few survivors thrive well in the second niche and reach giant sizes (Fig. 2). This sudden change in asymptotic size corresponds to a fold bifurcation (see also Claessen *et al.*, in press).

An important general conclusion from Fig. 2 is that there is a strong ecological feedback between the niche switch size u and the environment (F_1 and F_2 equilibrium densities). Changing u may drastically change prey densities, which, in turn, may change predator population density and individual growth rates. Comparison of Fig. 2a with Fig. 2b suggests that specific choices for the parameters of the size scaling of the functional response do not affect the general pattern. We have studied many different parameter combinations of a_1, a_2, h_1, h_2, p, q_1 and q_2 and all give the same overall pattern as illustrated in Fig. 2.

PAIRWISE INVASIBILITY PLOTS

This section briefly outlines the methodology and terminology that we use in our study of the evolution of the switch size u. Our evolutionary analysis of the deterministic model is based on the assumptions that (1) mutations occur rarely, (2) mutation steps are small and (3) successful invasion implies replacement of the resident type by the mutant type. The robustness of these assumptions will be evaluated later (see pp. 208–210). Under these assumptions, evolution boils down to a sequence of trait substitutions. To study this, we consider a monomorphic resident population with genotype u and determine the invasion fitness of mutants, whose strategy we denote u'. With our model of the ecological interactions (see previous section on 'Ecological dynamics'), we can determine the fitness of a mutant type from the food densities F_1 and F_2, as is shown on pp. 200–201. Since the food densities are set by the resident population, the fitness of mutants depends on the strategy of the resident. If the lifetime reproduction, R_0, of a mutant exceeds unity, it has a probability of invading and replacing the resident (Metz *et al.*, 1992).

For all possible pairs of mutants and residents, the expected success of invasion by the mutant into the ecological equilibrium of the resident can be summarized in a so-called pairwise invasibility plot (van Tienderen and de Jong, 1986). For example, Fig. 3a is a pairwise invasibility plot for residents and mutants in the range of switch sizes from 0 to 2 cm, based on our model (Table 2). It shows that, if we choose a resident with a very small switch size, say $u = 0.1$, all mutants with a larger trait value ($u' > u$) have the possibility to invade the resident, whereas mutants with a smaller trait value ($u' < u$) have a negative invasion fitness and hence cannot establish themselves. Thus, the resident is predicted to be replaced by a mutant with a larger switch size. Upon establishment, this mutant becomes the new resident and the pairwise invasibility plot can be used to predict the next trait substitution. Figure 3a shows that, as long as the resident type is below u^*, only mutants with a larger trait value ($u' > u$) can invade. Thus, if we start with a resident type below u^*, the adaptive process results in a stepwise increase of the resident trait value towards u^*. A similar reasoning applies to the residents with a trait value above u^*. Here, only mutants with a smaller switch size can invade (Fig. 3a). Therefore, starting from any initial resident type near u^*, the adaptive process results in convergence of the resident to u^*. The strategy u^* is hence an evolutionary attractor.

In a pairwise invasibility plot, the borders between areas with positive and negative invasion fitness correspond to zero fitness contour lines. The diagonal ($u' = u$) is necessarily a contour line because mutants with the same strategy as the resident have the same fitness as the resident. Intersections of other contour lines with the diagonal are referred to as evolutionarily singular points (e.g. u^*). Above, we used the pairwise invasibility plot to determine the convergence stability of u^*, but we can also use it to determine the evolutionary stability of singular points. For example, Fig. 3a shows that if the resident has strategy u^*, all mutant strategies $u' \neq u$ have negative invasion fitness. A resident with switch size u^* is therefore immune to invasion by neighbouring mutant types and it is thus an evolutionarily stable strategy (ESS). A singular point that is both convergence stable and evolutionarily stable is referred to as a continuously stable strategy (CSS; Eshel, 1983).

In general, the dynamic properties of evolutionarily singular points can be determined from the slope of the off-diagonal contour line near the singular point (Metz *et al.*, 1996a; Dieckmann, 1997; Geritz *et al.*, 1998). In our analysis below, we find four different types of singular points. As we showed above, u^* in Fig. 3a corresponds to a CSS. In Fig. 3b, the

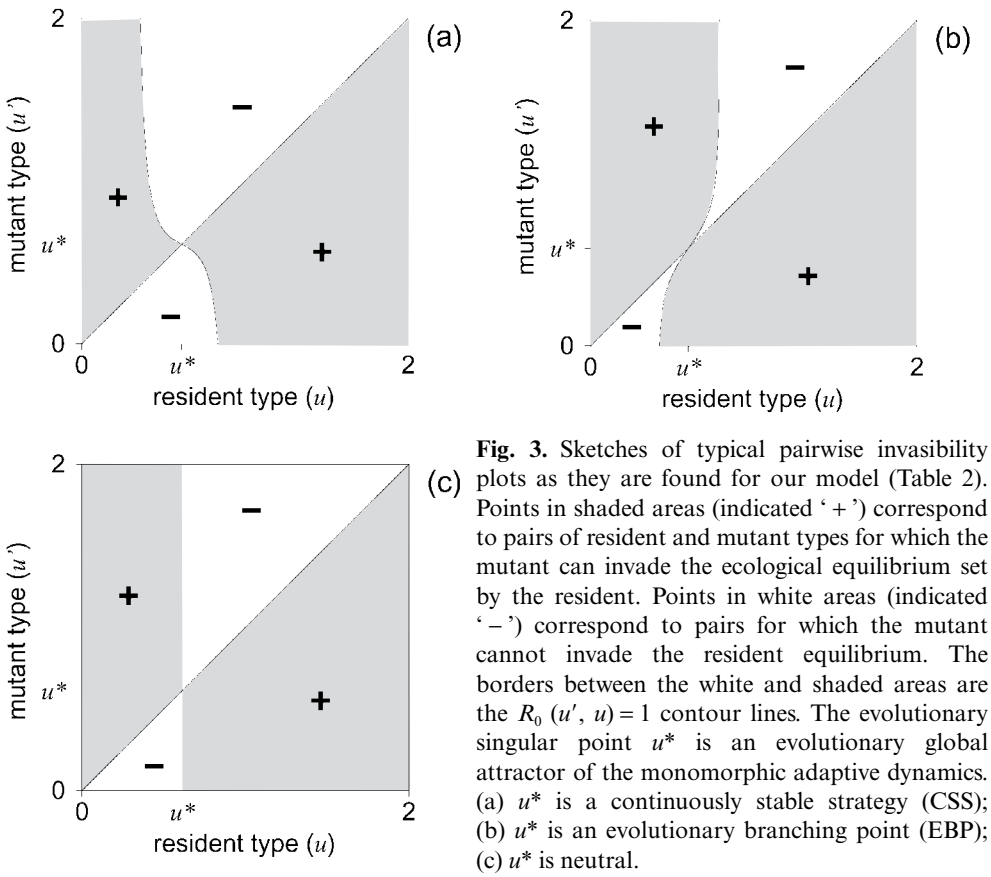

Fig. 3. Sketches of typical pairwise invasibility plots as they are found for our model (Table 2). Points in shaded areas (indicated ' + ') correspond to pairs of resident and mutant types for which the mutant can invade the ecological equilibrium set by the resident. Points in white areas (indicated ' − ') correspond to pairs for which the mutant cannot invade the resident equilibrium. The borders between the white and shaded areas are the $R_0\,(u', u) = 1$ contour lines. The evolutionary singular point u^* is an evolutionary global attractor of the monomorphic adaptive dynamics. (a) u^* is a continuously stable strategy (CSS); (b) u^* is an evolutionary branching point (EBP); (c) u^* is neutral.

singular point u^* is again an evolutionary attractor. However, once a resident population with strategy u^* has established itself, mutants on either side of the resident (i.e. both $u' > u$ and $u' < u$) have positive fitness. Since mutants with the same strategy as the resident have zero invasion fitness, the singular point u^* is located at a fitness minimum. It should be pointed out here that, under frequency-dependent selection, evolutionary stability and evolutionary convergence (or attainability) are completely independent (Eshel, 1983). In spite of being a fitness minimum, the strategy u^* in Fig. 3b is nevertheless an evolutionary attractor. As will become clear below (see pp. 208–210), a singular point that is convergence stable but evolutionarily unstable (e.g. u^* in Fig. 3b) is referred to as an evolutionary branching point (Metz *et al.*, 1996a; Geritz *et al.*, 1997).

In Fig. 3c, the singular point u^* is also an evolutionary attractor, but it is evolutionarily neutral; if the resident is u^*, all mutants have zero invasion fitness. We consider it a degenerate case, because even the slightest perturbation results in the situation of Fig. 3a or Fig. 3b.

The last type of singular point that we will encounter is illustrated in Fig. 4. In these pairwise invasibility plots, there are two evolutionarily singular points, of which u^* is an evolutionary branching point. From the sign of the invasion fitness function around the singular point u_r, we can see that if we start with a resident close to the singular point,

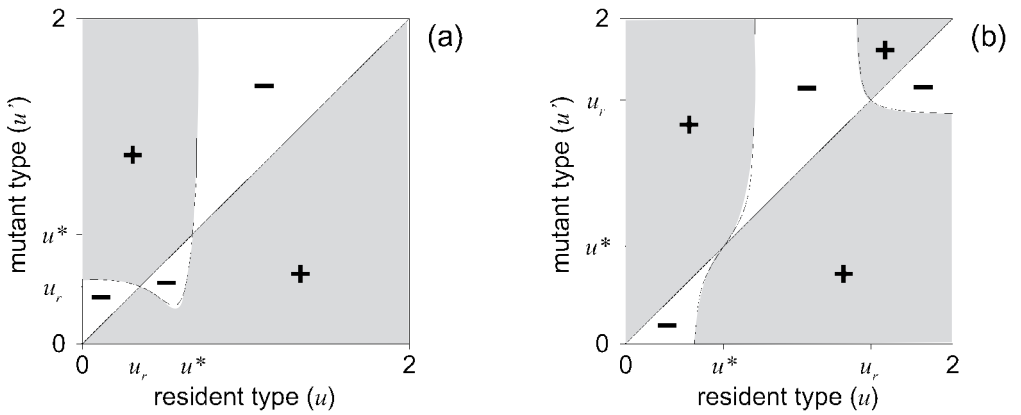

Fig. 4. Sketches of two additional pairwise invasibility plots that are found for our model (Table 2). Points in shaded areas (indicated ' + ') correspond to pairs of resident and mutant types for which the mutant can invade the ecological equilibrium set by the resident. Points in white areas (indicated ' – ') correspond to pairs for which the mutant cannot invade the resident equilibrium. The borders between the white and shaded areas are the $R_0(u', u) = 1$ contour lines. The singular point u^* is an evolutionary branching point (EBP). The singular point u_r is an evolutionary repeller. We find (a) if prey 1 is very hard to digest (high h_1) and (b) if prey 2 is very hard to digest (high h_2).

mutants with a strategy even closer to u_r cannot invade. Rather, successful invaders lie further away from u_r. Trait substitutions are hence expected to result in evolution away from u_r. Singular points such as u_r in Fig. 4 are convergence unstable and are referred to as evolutionary repellers (Metz *et al.*, 1996a).

EVOLUTIONARY DYNAMICS

In this section, we study the evolution of the size at niche shift (u) within the ecological context established in the section on 'Ecological dynamics'. First, we use the deterministic model to find evolutionarily singular points and their dynamic properties, using the method outlined in the previous section. Second, we interpret them in terms of ecological mechanisms. Third, we use numerical simulations of a stochastic individual-based version of the same model to check the robustness of the derived predictions.

Invasion fitness of mutants

We first have to determine the fitness of mutants as a function of their own switch size u' and of the the resident's switch size u. With our individual-level model (see section on 'Ecological dynamics'), we can relate the lifetime reproduction, R_0, of a mutant to its strategy. We can use R_0 as a measure of invasion fitness, because a monomorphic resident population with strategy u can be invaded by mutants with strategy u' if the expected lifetime reproduction of the mutant in the environment set by the resident exceeds unity – that is, if $R_0(u', u) > 1$ (Mylius and Diekmann, 1995).

The environment that a mutant experiences consists of the two prey densities, which are in equilibrium with the resident population, so we write $F_1(u)$ and $F_2(u)$. The mutant's

length–age relation can be obtained by integration of equation (10) after substitution of $F_1(u)$ and $F_2(u)$. Knowing the growth trajectory, the birth rate as a function of age can be calculated from equation (9). We denote this age-specific birth rate by $B(a, u', u)$, where a denotes age. The mutant's lifetime reproduction R_0 is then found by integration of this function, weighted by the probability of surviving to age a, over its entire life history:

$$R_0(u', u) = \int_0^\infty \mathrm{e}^{-\mu a} B(a, u', u)\, \mathrm{d}a \tag{14}$$

Based on the assumption of size-independent mortality, $R_0(u', u)$ is a monotonically increasing function of the feeding rate at any size. The reason is straightforward: an increased feeding rate implies an increased instantaneous birth rate, as well as an increased growth rate. The size-specific birth rate b (equation 9) is monotonically increasing in x. These three facts imply that an increase in the intake rate at any size increases the lifetime reproduction (in a constant environment).

For each value of the resident's trait u from the range between the two specialist trait values ($u = 0 \ldots 4$), we numerically determine the function $R_0(u', u)$ for values of u' from the same range. The results of these calculations are summarized in pairwise invasibility plots (see pp. 198–200), which show the contour lines $R_0(u', u) = 1$ and the sign of $R_0(u', u) - 1$ (Figs 3 and 4).

The results for many different parameter combinations show that there are five qualitatively different pairwise invasibility plots, which are represented in Figs 3 and 4. All five pairwise invasibility plots have one important feature in common: there is an intermediate switch size that is an evolutionary attractor of the monomorphic adaptive dynamics. We denote this attractor by u^* and refer to it as the generalist strategy. In Fig. 3, u^* is a global attractor, whereas in Fig. 4 there is also an evolutionary repeller. Choosing a resident switch size beyond the repeller leads to evolution towards a single specialist population, leaving the other niche (the first niche in Fig. 4a; the second in Fig. 4b) unexploited. We first discuss the evolutionary attractor u^* and return to the evolutionary repellers later in the section.

Evolutionary convergence to the generalist u^*

Here we relate the results presented in Fig. 3 to the underlying ecological mechanisms. We can explain the different evolutionary outcomes by considering the life history of individuals in terms of their size-dependent food intake rate (equation 7). To clarify the ecological mechanism, we compare the size-dependent food intake rate of a resident individual with the *possible* intake rates in each niche separately (equation 8; Fig. 5). Thus, we gain insight into whether the actual intake rate at a certain size is above or below the possible intake rate at that size.

The length at which the possible intake rates $\hat{f}_1(x, F_1)$ and $\hat{f}_2(x, F_2)$ (equation 8) intersect is denoted x_e. This particular body length is of special interest, because one niche is more 'profitable' to individuals smaller than x_e, whereas the other niche is more profitable to individuals larger than x_e. Here, 'more profitable' is defined as 'providing a higher possible intake rate'. To an individual of length $x = x_e$, the two niches are hence equally profitable. Figure 5 illustrates that the evolutionary attractor u^* is that particular strategy for which the switch size u coincides with the intersection of the possible intake rates (i.e. $x_e = u$).

Depending on the size scaling of the two possible intake rates, two generic cases can be distinguished: (a) the first niche is more profitable than the second one to individuals

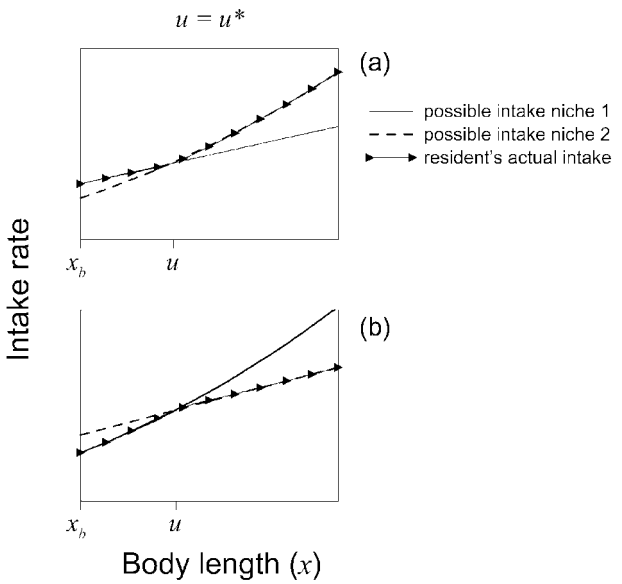

Fig. 5. Comparison of the size-dependent, *actual* intake rate of the resident with the *possible* intake rates in each niche separately, given the densities of F_2 and F_2 as set by the resident. The residents in (a) and (b) correspond to u^* in Fig. 3a and b, respectively. Note that the switch size u and the intersection of the two possible intake rates coincide. (a) Possible attack rate is proportional to body length in the first niche ($q_1 = 1$) and proportional to body surface area in the second ($q_2 = 2$); the resident ($u^* = 0.68$) is a continuously stable strategy (CSS). (b) Possible attack rate is proportional to body surface area in the first niche ($q_1 = 2$) and proportional to body length in the second ($q_2 = 1$); the resident ($u^* = 0.683$) is an evolutionary branching point (EBP). Other parameters: $k = 30$, $p = 2$, $a_1 = a_2 = 1$, $h_1 = h_2 = 10$ and as in Table 1.

smaller than x_e, but less profitable to individuals larger than x_e, and (b) vice versa. The two cases are illustrated in Fig. 5a and b, respectively. In the rest of this section (including the figures), we refer to these cases as case (a) and case (b). For comparison, Fig. 2 also shows cases (a) and (b).

Why u^* is an evolutionary attractor can be understood by considering a perturbation in the switch size u; that is, by choosing a resident strategy u slightly smaller or larger than u^*. In this case, the possible intake rates intersect at some body size $x_e \neq u$. In Fig. 6 (right-hand panels), the resident has a strategy slightly above the generalist strategy ($u > u^*$). Compared with Fig. 5, the curves of the two possible intake rates have shifted; $\hat{f}_1$ downward and $\hat{f}_2$ upward. The reason is that the prey densities F_1 and F_2 depend on the resident strategy u (Fig. 2). As a consequence, to an individual with length equal to the switch length ($x = u$), the second niche seems underexploited. We define the 'underexploited' niche as the niche that gives an individual of length $x = u$ the highest possible intake rate (equation 8). The other niche is referred to as 'overexploited'.

Now, consider a mutant with a strategy u' in the environment set by a resident with $u > u^*$. If the mutant has a smaller switch size than the resident, it switches to the underexploited niche before the resident does. Its intake rate, therefore, is higher than the resident's intake and, since fitness increases monotonically with the intake rate, the mutant can

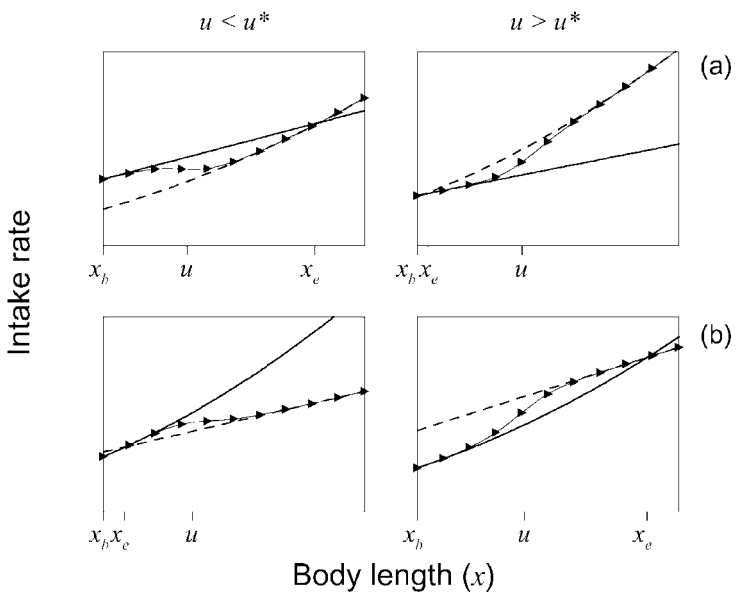

Fig. 6. Perturbations in the switch size u. For cases (a) and (b) depicted in Fig. 5, a resident was chosen just below the singular point ($u < u^*$) and one resident just above it ($u > u^*$). Assuming the ecological equilibrium of these residents, the actual and possible intake rates are plotted (legend: see Fig. 5). x_e marks the length at which the possible intake rates intersect. Parameters: (a) $q_1 = 1$, $q_2 = 2$. (b) $q_1 = 2$, $q_2 = 1$. Other parameters as in Fig. 5.

invade. Mutants that switch later than the resident, however, spend more time in the overexploited niche, have a lower intake rate and hence cannot invade. This shows how natural selection drives the system in the direction of the generalist u^* when started from a resident with $u > u^*$.

For the case $u < u^*$, the opposite reasoning applies: a resident that switches between niches at a relatively small size underexploits the first niche and overexploits the second one. The curve describing the possible intake rate in the first niche ($\hat{f}_1$) shifts upward, whereas the curve for the second niche ($\hat{f}_2$) shifts downward (Fig. 6, left-hand panels). Only mutants that switch later ($u' > u$) profit more from the underexploited niche than the resident, and hence only these mutants can invade, such that evolution moves the system towards the generalist u^* when started from a resident with $u < u^*$.

In summary, if one niche is underexploited, natural selection favours mutants that exploit this niche more. In consequence, only mutants that are closer to the generalist strategy u^* than the resident can invade. This suggests that u^* is an evolutionary attractor. Convergence to u^*, however, also depends on the effect of the environmental feedback on x_e. That is, once an invading strategy has replaced the old resident, it gives rise to a new ecological equilibrium. Because x_e depends on the prey densities F_1 and F_2, we need to check the relation between resident switch size u and the resultant x_e.

Again, we have to distinguish between cases (a) and (b) because the slopes of the possible intake rates at their intersection are crucial. Figure 6 shows that in case (a) the second niche is underexploited if $x_e < u$ and overexploited if $x_e > u$. This means that evolutionary

convergence to u^* is guaranteed if all residents with $u > u^*$ have an intersection point $x_e < u$ and all residents with $u < u^*$ have an intersection point $x_e > u$. Figure 7a shows that this is indeed the case. In case (b), the second niche is underexploited if $x_e > u$ and overexploited if $x_e < u$. For convergence to u^*, the relation between x_e and u should hence be opposite to case (a); Fig. 7 confirms that this applies. The relations in Fig. 7, and hence convergence to u^*, hold as long as the following condition is fulfilled at $u = u^*$:

$$\left.\frac{\partial \hat{f}_1}{\partial u}\right|_{x=u} < \left.\frac{\partial \hat{f}_2}{\partial u}\right|_{x=u}$$

Although we cannot prove that this condition is met in general, intensive numerical investigations have found no exception for any parameter combinations. We conjecture that the inequality above can be taken for granted if the following, more elementary, condition is fulfilled at $u = u^*$:

$$\frac{\partial F_1}{\partial u} < \frac{\partial F_2}{\partial u}$$

Evolutionary stability of the generalist u^*

The pairwise invasibility plots (Fig. 3) suggest that the evolutionary attractor u^* is either a continuously stable strategy (CSS), an evolutionary branching point (EBP) or neutral. Which of these cases applies depends on the size scaling of the possible intake rates in the two niches. We show this by considering the two generic possibilities in Fig. 5, starting with case (a). For a resident that is smaller than its switch size, the first niche is more profitable than the second – that is, $\hat{f}_1(x) > \hat{f}_2(x)$ for $x < u$ (Fig. 5a). Consequently, mutants that switch

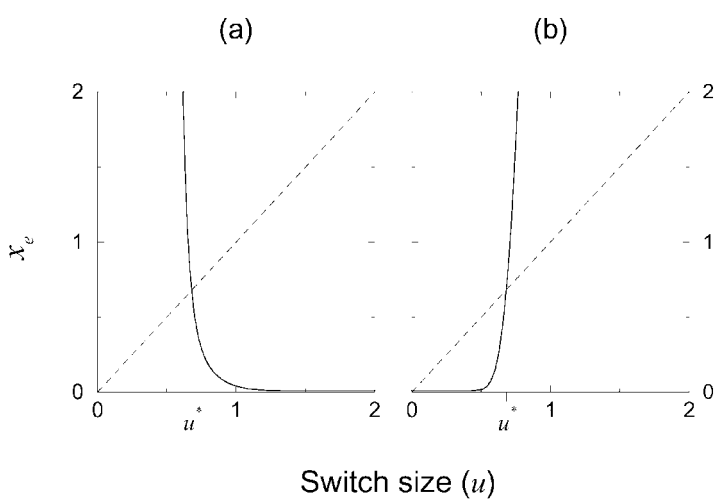

Fig. 7. The environmental feedback represented by the body length for which the two niches are equally profitable (x_e) as a function of the resident switch length (u). (a) and (b) as in Fig. 5 and Fig. 6. The switch size for which $x_e = u$ is referred to as the generalist strategy, denoted u^*. In (a) $u^* = 0.68$ and in (b) $u^* = 0.683$.

earlier than the resident ($u' < u$) switch to the second niche at a size at which the second niche is still less profitable to them than the first. They hence have lower fitness than the resident. For individuals larger than the resident switch size, the second niche is more profitable than the first – that is, $\hat{f}_2(x) > \hat{f}_1(x)$ for $x > u$. This implies that mutants that switch later than the resident ($u' > u$) stay in the first niche, although this niche has become less profitable to them than the second one. These mutants, too, have lower fitness than the resident. Since mutants on both sides of the resident strategy cannot invade, the generalist u^* is a CSS.

Case (b) is simply the opposite of the previous case. The first niche is less profitable to individuals smaller than the switch size, whereas the second niche is less profitable to individuals larger than the switch size. As a consequence, mutants that switch earlier ($u' < u$) switch to the second niche while it still is more profitable to them. Mutants that switch later ($u' > u$) stay in the first niche when it becomes more profitable to them. The evolutionary attractor u^* thus lies at a fitness minimum and, since it is nevertheless convergence stable, it is an evolutionary branching point.

Which biological conditions give rise to cases (a) and (b)? In the next two subsections, we derive conditions for theses cases in terms of our model parameters; this allows for a qualitative comparison between our results and empirical data on the size scaling of functional responses. To aid our biological interpretation of the results and because of the complexity of equation (7), we apply two alternative simplifying assumptions. In a first scenario, we assume that the handling times for the two prey types are equal ($h_1 = h_2$). In a second scenario, we consider different handling times, but assume the same possible attack rates in both niches ($a_1 = a_2$, $q_1 = q_2$).

Scenario 1: different attack rates

Here, we assume that the only difference between the two niches is the size scaling of the possible attack rates, whereas handling times are assumed to be the same. In this case, we can find an explicit expression for the length x_e at which the two possible intake rates intersect. The intersection x_e is obtained by substituting $h_1 = h_2 = h$ in the possible intake rates (equation 8) and by solving for $\hat{f}_1(x) = \hat{f}_2(x)$:

$$x_e = \left(\frac{a_1 F_1}{a_2 F_2}\right)^{1/(q_2 - q_1)} \tag{15}$$

To distinguish between cases (a) and (b), we define a function $D(x)$ that is the difference between the possible intake rates in the two niches:

$$D(x) = \hat{f}_1(x) - \hat{f}_2(x) \tag{16}$$

In case (a), the first niche is more profitable before the switch, while the second one is more profitable after the switch; this requires that the slope of $D(x)$ evaluated at $x = x_e$ is negative. Case (b) results when the slope of $D(x)$ at size x_e is positive.

The function $D(x)$ can be written as

$$D(x) = \frac{a_1 F_1 x^{q_1} - a_2 F_2 x^{q_2}}{1 + a_1 F_1 x^{(q_1 - p)} h + a_2 F_2 x^{(q_2 - p)} h + a_1 F_1 a_2 F_2 x^{(q_1 - 2p + q_2)} h^2} \tag{17}$$

By definition, $D(x_e) = 0$, so we only have to consider the sign of $D(x)$ around $x = x_e$. Since the denominator of equation (17) is always positive, we have to determine the sign of the numerator only. The numerator is positive for a length x between 0 and x_e if, and only if, $q_1 < q_2$. Thus we arrive at the conditions:

$$\begin{aligned} q_1 < q_2 \quad & \text{CSS} \\ q_1 = q_2 \quad & \text{neutral} \\ q_1 > q_2 \quad & \text{EBP} \end{aligned} \tag{18}$$

If the possible attack rate on the first prey type increases faster with body size than the possible attack rate on the second prey type (Fig. 5b), the evolutionary attractor u^* is predicted to be an evolutionary branching point (Fig. 3b). Otherwise, the generalist is predicted to be a CSS or to be neutral and the population to remain monomorphic. Note that Fig. 2, Fig. 5 and Fig. 7 illustrate this first scenario.

Scenario 2: different handling times

Here, we assume that the possible attack rates are the same (i.e. $a_1 = a_2 = a$, $q_1 = q_2 = q$), but that the two prey types differ in digestibility (i.e. $h_1 \neq h_2$). The reasoning is analogous to that applied in the first scenario. The length at which the niches are equally profitable is:

$$x_e = \left(\frac{F_1 - F_2}{aF_1F_2(h_1 - h_2)} \right)^{1/(q-p)} \tag{19}$$

The difference between the possible intake rates is:

$$D(x) = \frac{ax^q[(h_2 - h_1)aF_1F_2x^{q-p} + F_1 - F_2]}{(1 + ax^{q-p}h_1F_1)(1 + ax^{q-p}h_2F_2)} \tag{20}$$

Again, the denominator is always positive, so we consider the numerator only. Here it is crucial to recognize that $D(x)$ is increasing if

$$(h_2 - h_1)aF_1F_2x^{q-p} \tag{21}$$

is increasing in x. Since x^{q-p} is increasing in x if $p < q$ and decreasing if $p > q$, we arrive at the following conditions for the evolutionary stability of the generalist u^*:

$$\begin{aligned} p > q \text{ and } h_1 < h_2 \quad & \text{CSS} \\ p < q \text{ and } h_1 > h_2 \quad & \text{CSS} \\ p = q \text{ or } h_1 = h_2 \quad & \text{neutral} \\ p > q \text{ and } h_1 > h_2 \quad & \text{EBP} \\ p < q \text{ and } h_1 < h_2 \quad & \text{EBP} \end{aligned} \tag{22}$$

Interpretation of these conditions is less obvious than for the first scenario and requires consideration of the size-dependent functional response (equation 7). If $p > q$, the maximum intake rate on a pure diet of prey i, $H_i(x)^{-1}$, increases faster with body size than the search rate. This means that, with increasing body size, the feeding rate becomes less

limited by digestive constraints and more limited by prey abundance. This can be clarified by the case of a single prey population, assuming a constant prey density F. Dividing the functional response f by the maximum intake rate, $H(x)^{-1}$, we obtain the level of saturation as a function of body size:

$$\left(\frac{1}{ahF}x^{p-q}+1\right)^{-1} \tag{23}$$

which is a decreasing function of x if $p > q$ and an increasing one if $p < q$. If the feeding rate is well below its maximum, the intake rate correlates strongly with the encounter rate between predator and prey, and the individual is 'search limited'. If, on the other hand, the feeding rate is close to its maximum, the intake rate correlates weakly with prey abundance, and individuals are 'handling limited'. For $p = q$, the level of saturation is independent of body size (like, for example, in the Kooijman-Metz model with $p = q = 2$).

Recall that, for a resident of size $x = u^*$, the two prey types are equally profitable (Fig. 5). If the feeding rate becomes more handling limited with body size ($p < q$), then for individuals larger than u^*, the prey that is more digestible (smaller h_i) is the more profitable one. If, on the other hand, the feeding rate becomes more search limited with body size, then for larger individuals, the more abundant prey (higher F_i) is more profitable. Rewriting equation (19) gives a relation between the prey densities at equilibrium of the resident population with switch size u^*:

$$F_2 = \frac{F_1}{1+(h_1-h_2)aF_1x_e^{q-p}} \tag{24}$$

This implies that the less digestible prey is the more abundant prey:

$$h_1 > h_2 \Leftrightarrow F_1 > F_2 \qquad \text{at } u = u^* \tag{25}$$

We first investigate the case $h_1 > h_2$, $p < q$, and consider a resident population with the singular strategy $u = u^*$ and a mutant that switches at a larger size than the resident ($u' > u$). In the size interval between the resident's switch size u and its own switch size u', the resident shifts its focus to prey 2 while the mutant is still focusing on prey 1. The mutant thus consumes the less digestible prey while it is relatively handling limited (relative to the size at which the two prey are equally profitable, u^*). Its intake rate is therefore smaller than that of the resident and hence also its lifetime reproduction. A mutant that switches at a smaller size than the resident ($u' < u$) consumes the less abundant prey 2 already at a size where it is relatively search limited. Also, this mutant has a smaller R_0 than the resident. Since mutants with $u' > u$ or $u' < u$ both cannot invade, the singular strategy u^* is a CSS if $h_1 > h_2$ and $p < q$. For $h_1 < h_2$ and $p > q$, an analogous reasoning applies.

We now consider the case $h_1 > h_2$ and $p > q$. A mutant that switches at a larger size continues consuming the more abundant prey 1 while it is relatively search limited, yielding a higher feeding rate and hence a higher fitness than the resident. A mutant that switches at a smaller size starts consuming the more digestible prey 2 while it is relatively handling limited, also yielding a higher fitness than the resident. Thus, mutations in both directions yield a higher fitness than the resident, which implies that the singular strategy is a branching point. Again, a completely analogous reasoning applies for $h_1 < h_2$ and $p < q$.

Evolutionary repellers

Under the assumptions that $a_1 = a_2 = a$ and $q_1 = q_2 = q$, we have identified parameter configurations leading to two singular points, where one is the generalist strategy u^* and the other is an evolutionary repeller (Fig. 4a,b). A repeller occurs at a small trait value if $p > q$ and h_1 is sufficiently high (Fig. 4a). In contrast, a repeller occurs at a large trait value if $p < q$ and h_2 is sufficiently high (Fig. 4b). In the latter case, if the population starts out with a trait value above the repeller, directional selection moves the population away from u^* and towards the strategy that is a specialist on prey 1. It is interesting to note – and, because of the asymptotic shape of the sigmoidal functions (Fig. 1), also biologically expected – that the fitness gradient goes asymptotically to zero as the resident switch size becomes larger. Similarly, starting below the repeller in the case with $p > q$, the population evolves to a specialist on prey 2, leaving the first prey unexploited. The existence of the repellers relates to the fact that, for severely handling-limited individuals, the less digestible prey type can be less profitable than the more digestible prey type even if the former's density is at its carrying capacity and the latter's density is low.

After branching: dimorphism of switch sizes

What happens after the adaptive dynamics of switch sizes has reached an evolutionary branching point, such as u^* in Fig. 3b? Mutants on either side of u^* can invade the resident population, which may give rise to the establishment of two (slightly more specialized) branches and exclusion of the generalist u^* (Metz *et al.*, 1996a; Geritz *et al.*, 1997). Whether the branches can co-exist depends on whether they can invade into each other's monomorphic equilibrium population. The set of u' and u strategies that can mutually invade is referred to as the set of protected dimorphisms. This set is found by flipping the pairwise invasibility plot (Fig. 3b) around the diagonal $u' = u$ (corresponding to a role reversal of the two considered strategies) and superimposing it on the original (Geritz *et al.*, 1998): combinations of strategies (u, u') for which the sign of $R_0(u', u) - 1$ before and after the flip is positive are protected dimorphisms and can co-exist. The set of protected dimorphisms in the vicinity of the branching point u^* is referred to as the co-existence cone and its shape has implications for the adaptive dynamics after branching. Specifically, the width of the cone determines the likelihood that evolutionary branching occurs and that the two branches persist: branching is more likely if the cone is wide. The reason is that mutation-limited evolution can be seen as a sequence of trait substitutions, which behaves like a directed random walk (Metz *et al.*, 1992; Dieckmann and Law, 1996). Due to the stochastic nature of this process, there is a probability of hitting the boundary of the co-existence cone, which results in the extinction of one of the two branches. The co-existence cone is wider the smaller the acute angle between the two contour lines at their intersection point u^*. In our model, this angle depends on the abruptness of the ontogenetic switch. If the shift is more gradual (corresponding to a lower value of k), the angle is smaller and, consequently, the co-existence cone is wider. Hence, with a gradual niche shift, evolutionary branching is more likely to occur than with a more discrete switch.

To determine whether our results are robust against relaxing some of the simplifying assumptions inherent to the deterministic, monomorphic model considered in this article up to now, we investigate a stochastic, individual-based model (IBM) that corresponds to the deterministic model (Tables 2 and 3). In the IBM, the growth dynamic of individuals is

still deterministic, but birth and death are modelled as discrete events. An offspring receives the same trait value as its clonal parents unless a mutation occurs, which we assume to occur with a fixed probability of $P = 0.1$ per offspring. The offspring's trait value is then drawn from a truncated normal distribution around the parental trait value. The standard deviation of the mutation distribution can be varied (we have considered values between 0.001 and 0.01). An essential feature of the IBM, and a major difference with the deterministic model studied above, is that it naturally allows for polymorphism to arise.

Convergence to the predicted singular point u^* and the subsequent emergence of a switch-size dimorphism in simulations of the IBM (e.g. Fig. 8) confirm the robustness of the results derived from the deterministic model. In particular, this shows that the assumption in our deterministic model that the strategy of offspring is identical to their parents' strategy is not critical to the results. The stochastic IBM has been studied for many different parameter combinations, and branching occurs only in runs with parameter settings for which this is predicted by the deterministic model (cf. conditions 18 and 22). Secondary branching, potentially giving rise to greater polymorphism, has not been observed.

The IBM allows us to study the evolution of the ontogenetic niche shift after branching. We will refer to the two emerging branches as A and B and denote the average switch sizes in the two branches as u_A and u_B, respectively, such that $u_A > u_B$ (Fig. 8). Figure 8 illustrates that the branches in the dimorphic population evolve towards two specialist strategies. Switch size u_A approaches the maximum size x_{max}, such that virtually all A-individuals consume prey 1 exclusively. Switch size u_B approaches the length at birth (x_b), such that individuals in branch B consume prey 2 throughout their entire lives. Prey densities remain approximately constant after branching. With constant prey densities, the possible intake rates are also constant, and this observation enables us to use Fig. 5b to understand the mechanism of divergence. Individuals in branch A have a switch size $u_A > u^*$. Figure 5b shows that, for individuals with a length (x) larger than the switch size u^*, the possible

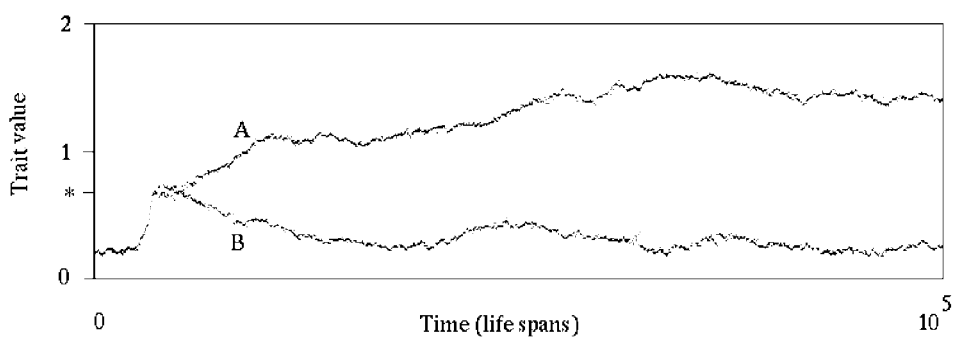

Fig. 8. A realization of a stochastic, individual-based implementation of our model. The population started out as a monomorphic specialist in niche 2 with $u = 0.2$ and first evolves towards the generalist strategy u^* ($u^* = 0.683$ predicted by the deterministic model; Fig. 5b). This singular point is a branching point. After branching, the two branches (denoted A and B) in the dimorphic population evolve towards the two specialist strategies, specializing on prey 1 (branch A) and prey 2 (branch B), respectively. Parameters as in Fig. 2b ($p = 2$, $q_1 = 2$, $q_2 = 1$, $a_1 = a_2 = 1$, $h_1 = h_2 = 10$, $k = 30$, Table 1). Mutation probability = 0.1, mutation distribution standard deviation = 0.003. Unit of time axis is $\mu^{-1} = 10$ time units.

intake rate is higher in the first niche than in the second. Therefore, mutants with a strategy $u' > u_A$ profit more from the first niche than A-type residents and can hence invade. Mutants with a strategy $u^* < u' < u_A$ suffer from their earlier switch to the less profitable niche and thus do not invade. In branch B, the situation is similar. For small individuals ($x < u^*$), the second niche is more profitable than the first one. Hence, mutants that switch earlier than B-type residents can invade the system, whereas mutants with a strategy $u_B < u' < u^*$ suffer from a diminished intake rate. In summary, the whole range of mutant trait values in between the two resident types ($u' = u_B \ldots u_A$) have a lower fitness than both residents. Only mutants outside this interval can invade, resulting in the divergence of branches A and B.

The results from the polymorphic, stochastic model were complemented by an analysis of an extension of our deterministic model that allows for dimorphism in the switch size of the predator population. This model predicts that, after branching, the two branches continue to diverge from each other at a decelerating rate (results not shown). The analysis also confirms that the prey densities remain approximately constant after branching. Further branching is not predicted by this model; in general, in a two-dimensional environment (resulting from the density of the predator population being regulated through two prey types at equilibrium), more than two branches are not expected (Metz *et al.*, 1996b; Meszéna and Metz, 1999). We can therefore conclude that Fig. 8 illustrates a typical scenario where a specialist first 'invades' the unexploited niche, then evolves towards the generalist strategy u^*, whereupon the population branches into two specialists.

DISCUSSION

Our results show that the presence of an ontogenetic niche shift in an organism's life history may give rise to evolutionary branching. The size scaling of foraging capacity in the two niches determines whether the predicted outcome of evolution is a monomorphic, ontogenetic generalist or a resource polymorphism with two 'morphs' specializing on one of two niches. A generalist is expected if the *possible* intake rate increases slower with body size in the first niche than in the second one (case a in Fig. 3a and Fig. 5a). In contrast, the evolutionary emergence of two specialists is predicted if the possible intake rate increases faster with body size in the first niche than in the second one (case b in Fig. 3b and Fig. 5b).

Mechanisms of evolutionary branching

Previous studies of ontogenetic niche shifts have mainly focused on the question *when* to make the transition between niches, given certain environmental conditions in terms of growth rates and mortality risks in two habitats (Werner and Gilliam, 1984; Werner and Hall, 1988; Persson and Greenberg, 1990; Leonardsson, 1991). With such an approach, one is unlikely to predict disruptive selection, because the environmental conditions that result in disruptive selection are rather special. Previous studies did not include the ecological feedback loop in their analysis. They considered the effect of the environment on individual life histories but neglected the effect of the size-structured population on the environment. In this study, we have shown that, through the effect of the ontogenetic niche shift on prey densities, evolution of the size at ontogenetic niche shift converges towards a generalist strategy that exploits both niches equally (u^*). This result is important, because only the environmental conditions associated with u^* have the potential to result in disruptive selection and, consequently, in evolutionary branching. Hence, despite the environmental

conditions for disruptive selection being rather special, it turns out that they are likely to arise because they correspond to an evolutionary attractor of the adaptive process.

Regarding the ecological mechanisms that drive evolution, our results show a clear dichotomy between two phases of evolution. As long as a monomorphic predator population consumes one prey type disproportionately, one niche is overexploited while the other remains underexploited. Mutants that utilize the unexploited prey more thoroughly can invade the system. As the predator's strategy evolves towards the generalist strategy u^*, the two niches become more and more equally exploited, and the selection gradient becomes weaker. Hence, during the initial, monomorphic phase, it is the environmental feedback that drives evolution towards the generalist strategy u^*. This process does not depend qualitatively on the size scaling of the functional response in the two niches.

In the second phase, after the population has reached the generalist strategy u^*, the size scaling of foraging rates determines the evolutionary stability of u^* (e.g. equation 18). If u^* is a continuously stable strategy (CSS; Fig. 3a), the resident population remains a monomorphic generalist. In contrast, if u^* is an evolutionary branching point (EBP; Fig. 3b), the resident population splits into two branches. In each branch, more specialized mutants can invade and replace the resident and hence the two branches diverge (Fig. 8). Why more specialized mutants can invade is explained by essentially the same mechanism as why u^* is an evolutionary branching point (cf. Fig. 5b). Crucial to the mechanism is that, given the ambient prey densities, the first niche is less profitable than the second one to individuals with a size smaller than u^*, and the second niche is less profitable than the first one to individuals with a size larger than u^*. In other words, individuals with the strategy u^* are in the least profitable niche at all sizes, whereas strategies that are different from u^* spent at least part of their lives in the most profitable niche. It is important to note that the difference in profitability of the two niches results from the size scaling of the functional response. Hence, in the second phase, the driving force of evolution relates critically to size structure. However, the ecological feedback and the resultant frequency-dependent selection remain important. If, for example, branch A were removed from the lake, branch B would evolve back to u^*.

As summarized above, we have found an ecological mechanism for evolutionary branching that is inherently size dependent. One way to show that size structure is essential to evolutionary branching is to show that it cannot occur in an analogous, unstructured model. If we just consider the fraction of lifetime that individuals spend in each niche and ignore all other aspects of the population size structure, we can formulate an unstructured analogue of our model. Analysis of such a model indicates that the environmental feedback drives evolution to a generalist strategy, analogous to the strategy u^* in the size-structured model (D. Claessen, unpublished results). With a linear functional response, this singular point is evolutionarily neutral (such as Fig. 3c). The reason is that, in the ecological equilibrium of this strategy, the two niches are equally profitable. By definition, if the niches are equally profitable, it does not matter which fraction of time individuals spend in each niche. With a Holling type II functional response, the evolutionary attractor can be either neutral or a CSS. Thus, in the simplest unstructured analogue of our model, evolutionary branching is not possible.

It should be noted, however, that evolutionary branching is possible in unstructured models of consumer–resource interactions with multiple resources. It can occur if there is a strong trade-off between foraging rates on different prey types (Egas, 2002). The essence of a strong trade-off is that, given prey densities, a generalist has a lower total intake rate

and hence lower fitness than more specialized strategies (Wilson and Yoshimura, 1994). With a weak trade-off, generalists have a higher intake rate than more specialized strategies and branching is not expected. In the unstructured analogue of our model, the time budget argument (i.e. defining the evolutionary trait as merely the fraction of lifetime spent in either niche) does not lead to a strong trade-off. For example, with a linear functional response, the trade-off is perfectly neutral because the actual food intake rate is merely a weighted average of the possible intake rates in the two niches. To obtain a strong trade-off, additional assumptions have to be made. It has been suggested that trade-offs may result from physiological or behavioural specialization (Schluter, 1995; Hjelm *et al.*, 2000; Egas, 2002). An example that is particularly relevant to this article is the possibility that learning or phenotypic plasticity produces a positive correlation between the foraging efficiency in a niche and the total time spent in that niche (e.g. Schluter, 1995). If such a correlation exists, generalists are at a disadvantage because they have less time to learn or to adapt to a specific food type. With this additional mechanism, branching may be expected even without size structure (D. Claessen, unpublished results).

The comparison with unstructured population models suggests that, on a phenomenological level, a strong trade-off emerges from our assumptions about the ontogenetic niche shift: the generalist u^* has a lower fitness than more specialized strategies. Our mechanistic modelling approach allows us to identify aspects of the underlying biology that are responsible for the strong trade-off. Critical to the mechanism of evolutionary branching in our model is the constraint of the order of niche use; individuals utilize the first niche before the ontogenetic niche shift and the second one after the niche shift. We assume that the order of niches is fixed by morphological development and physiological limitations. Evidence for such constraints includes, for example, that gape limitation prevents newborn perch to consume macroinvertebrates, whereas very large perch (longer than 20 cm) are not able to capture zooplankton prey, which has been attributed to insufficient visual acuity (Byström and Garcia-Berthou, 1999). Without the fixed order of niches, an individual would optimize its performance by always being in the niche that gives the highest possible intake rate, switching at the intersection point. As an example, consider a resident as depicted in Fig. 5b (i.e. an EBP) and a mutant that reverses the order of the ontogenetic niches, but still switches at length u. In this situation, the mutant can invade because its intake rate is higher than that of the resident at all sizes. When this mutant reaches fixation, we effectively obtain the situation as depicted in Fig. 5a. With this new order of ontogenetic niches, evolutionary branching is not expected. If the order of niches is also an evolutionary trait, as well as the switch size u, it is likely that the only possible evolutionary outcome is a monomorphic generalist (cf. the CSS in Fig. 5a). Thus, the constraint of the order of niches appears to be an essential element of our hypothesis that an ontogenetic niche shift can result in evolutionary branching.

Assumptions revisited

Several assumptions in our model are not very realistic and relaxing these may have important consequences for the predictions made. First, we assume that reproduction is clonal, which for all fish systems is unrealistic. In a randomly mating sexual population, the continual creation of hybrids may prevent evolutionary branching to occur. Yet, the study by Dieckmann and Doebeli (1999) shows that evolution itself may solve this problem, since once the population has evolved to the evolutionary branching point, natural selection

favours assortative mating (see also Geritz and Kisdi, 2000). Even if assortative mating is based on a character other than the ecological trait that has converged to the branching point, after a correlation between the ecological trait and the separate mating trait has been established, the population branches after all. Thus, we expect our results to be robust to the introduction of sexual reproduction in systems where assortative mating may arise. An example of the development of a correlation between ecological type and mating type (based on coloration) is the Midas cichlid (*Cichlasoma citrinellum*) (Meyer, 1990). Interestingly, the resource polymorphism in this species is associated with an ontogenetic niche shift. Wilson *et al.* (2000) argue that sexual selection through colour-based assortative mating is the primary reason for the polymorphism in this species. However, the appearance of colour-based assortative mating can also be a consequence of disruptive selection caused by ecological mechanisms such as described in this article. Such ecological differentiation might in fact be essential to ensure the sustained co-existence of colour morphs.

Second, we have assumed that individuals are born mature, which obviously is not the case in fish species. The presence of a juvenile period in size-structured populations can result in population cycles (Gurney and Nisbet, 1985; Persson *et al.*, 1998). The effect of non-equilibrium dynamics on evolution in our model remains to be investigated. A preliminary analysis shows that a sufficiently large maturation size threshold (> 10.5 cm) induces generation cycles. Less expected, however, is the result that for smaller values of the maturation size threshold, the juvenile delay introduces bistability through a cusp bifurcation (D. Claessen, unpublished results). Interestingly, the bistability gives rise to evolutionary cycling, in which the system never reaches the singular point u^*. Thus, a juvenile delay may drastically change the evolutionary outcome. These issues provide interesting questions for future research. It is encouraging, however, that with a sufficiently small value of the maturation size threshold (< 2 cm), our results remain unaffected, which shows that they are robust to incorporating a juvenile delay, at least as long as this does not give rise to population cycles or bistability.

Third, a basic assumption in our analysis is a niche- and size-independent mortality rate. Previous work on ontogenetic niche shifts (e.g. Werner and Hall, 1988) has often considered habitat choice within a trade-off between habitat-specific growth rates and mortality risks. Moreover, there is good evidence that, in many fish populations, mortality is inherently size-dependent, even if we disregard the effect of habitat. Important causes of such size dependence are overwintering mortality and size-dependent vulnerability to predation (Sogard, 1997). It is easy to incorporate niche- or size-dependent mortality into our model, but adding such realism comes at the cost of a clear interpretation. Preliminary analysis of a model that includes niche-dependent mortality shows that the same types of predictions are possible regarding the evolutionary outcomes (results not shown). However, the conditions and mechanisms underlying these predictions (cf. equations 18 and 22) are much less transparent. Instead of comparing possible intake rates at the switch size, as we did in this article, one must then compare the contributions to fitness over entire size intervals. Thus, for systems in which differences in niche-dependent mortality are large, conditions (18) and (22) should be regarded as approximations.

For the issue of size-dependent mortality, it is useful to distinguish between two general scenarios; depending on whether mortality rate (i) decreases or (ii) increases with body size. We argue that size-dependent mortality is likely to lead to qualitatively different results in scenario (ii) only. Underlying the results reported here is that fitness increases with the food intake rate at any given size in our model. The validity of this assumption may

break down if mortality rate increases with body size, since an increased food intake rate eventually leads to a higher mortality rate. In scenario (i), this assumption is not violated, since a higher growth rate improves future survival. Although the risk of predation is not necessarily a monotonic function of prey body size (Lundvall *et al.*, 1999), a general pattern in teleost fishes is that mortality decreases with body size (Sogard, 1997). We therefore argue that incorporating a realistic size-dependent mortality rate will not alter our results qualitatively.

The scope for empirical testing

With experimental data on size scaling of foraging rates, we can make predictions about whether or not evolutionary branching should be expected. For several reasons, freshwater fish populations are interesting test cases for the ideas developed in this article. The life history of freshwater fish species is often characterized by one or more ontogenetic niche shifts (Werner and Gilliam, 1984). Resource polymorphisms in several lake fish species have been suggested to represent early stages of speciation (Meyer, 1990; Smith and Skúlason, 1996). Most resource polymorphisms in lake-dwelling fish species involve a benthic morph and a pelagic morph (Robinson and Wilson, 1994). In Arctic char (*Salvelinus alpinus*; Snorrason *et al.*, 1994; Smith and Skúlason, 1996) and sticklebacks (*Gasterosteus aculeatus*; Schluter, 1996; Rundle *et al.*, 2000), empirical evidence suggests that evolutionary branching, giving rise to a benthic morph and a pelagic morph, has occurred several times independently.

Unfortunately, the number of species for which sufficient data on size scaling of foraging rates is available is still limited. Most detailed data exist for Eurasian perch (Byström and Garcia-Berthou, 1999; Wahlström *et al.*, 2000), roach (*Rutilus rutilus*; Persson *et al.*, 1998; Hjelm *et al.*, 2000) and bluegill sunfish (*Lepomis macrochirus*; Mittelbach, 1981). For perch and roach, the handling times can be assumed to be independent of prey type (Claessen *et al.*, 2000), such that scenario 1 (pp. 205–206) applies. Before the ontogenetic niche shift, perch and roach feed on zooplankton in the pelagic habitat; after the shift, they feed on macroinvertebrates in the littoral zone. For small individuals of both species, the attack rate on zooplankton scales approximately with body surface area (i.e. $q_1 \approx 2$). For larger individuals, the attack rate on macroinvertebrates scales roughly with length in perch (i.e. $q_2 \approx 1$; Persson and Greenberg, 1990) and is nearly constant in roach (i.e. $q_2 \approx 0.05$; J. Hjelm, personal communication). Bluegill sunfish switch from the littoral vegetation zone to the pelagic habitat at a length between 50 and 90 mm (Werner and Hall, 1988). In the former habitat they feed on macroinvertebrates and in the latter on zooplankton. Using data on the size scaling of encounter rates with prey from Mittelbach (1981), we arrive at estimates of $q_1 \approx 0.5$ and $q_2 \approx 2$ for bluegill.

This short inquiry of available data shows that there is at least the possibility of testing the results of our evolutionary analysis with empirical data. Although it is tempting to compare these data with conditions (18), we stress that, in spite of our model's complexity, it is still rather strategic. Rather than being designed for a specific ecological system, it is designed to test the effect of a specific mechanism. To keep it tractable, we have based our model on several simplifying assumptions, such as the absence of sexual reproduction, the absence of a juvenile delay and population dynamic equilibrium. We believe that a thorough empirical test of our model predictions would require either (a) an extension of our model, tailored specifically for a particular experimental set-up, or (b) data on a larger number

of species than are presently available, which would permit the emergence of general patterns.

Concerning point (a), obvious extensions of our model include sexual reproduction, size-dependent mortality and a juvenile period (see pp. 212–214). For example, this will have to show whether it matters that individuals mature before or after the ontogenetic niche shift. With regard to point (b), it should be noted that comparison of our conditions (equations 18 and 22) with empirical data ideally requires estimates of the *possible* intake rates. The size scalings of actual attack rates as presented above must be interpreted as fairly crude approximations, since they are confounded by the effect of the ontogenetic niche shift of the species. In Eurasian perch, for example, the relation between the attack rate on zooplankton and perch body size is dome-shaped. In our interpretation (and in our model; see equation 1), the attack rate on zooplankton declines at large body size because of morphological adaptation to an ontogenetic niche shift to benthivory (Hjelm *et al.*, 2000). One will have to make assumptions to filter out the effect of the ontogenetic niche shift on the *actual* attack rate function to arrive at an estimate of the *possible* attack rate function. Yet, in the case of a species pair which has diverged into specialists, the actual intake rate of a specialist in its preferred niche can be assumed to be a fair approximation of the possible intake rate. Candidate systems include Arctic char (Jonsson and Jonsson, 2001), sticklebacks (Schluter, 1996) and cichlids (Meyer, 1990; Schliewen *et al.*, 1994). Measurements of the size scaling of foraging rates in such systems would provide material for a critical test of our hypothesis.

ACKNOWLEDGEMENTS

This research was inspired by many discussions with Jens Andersson, Jocke Hjelm, Lennart Persson and Rickard Svanbäck, in Umeå. Most of the research reported here was done during the Young Scientist Summer Program (YSSP) in the Adaptive Dynamics Network (ADN) at the International Institute for Applied Systems Analysis (IIASA), Laxenburg, for which D.C. received a grant from the Dutch Science Foundation (NWO). During the YSSP, discussions with the other ADN students (Sondre Aanes, Fabio Dercole, Juan Keymer, Rahel Luethy, Christian Magori and Kalle Parvinen) were very stimulating.

REFERENCES

Byström, P. and Garcia-Berthou, E. 1999. Density dependent growth and size specific competitive interactions in young fish. *Oikos*, **86**: 217–232.

Claessen, D., de Roos, A.M. and Persson, L. 2000. Dwarfs and giants: cannibalism and competition in size-structured populations. *Am. Nat.*, **155**: 219–237.

Claessen, D., van Oss, C., de Roos, A.M. and Persson, L. in press. The impact of size-dependent predation on population dynamics and individual life history. *Ecology*.

de Roos, A.M. 1988. Numerical methods for structured population models: the Escalator Boxcar Train. *Numerical Methods for Partial Differential Equations*, **4**: 173–195.

de Roos, A.M. 1997. A gentle introduction to physiologically structured population models. In *Structured Population Models in Marine, Terrestrial, and Freshwater Systems* (H. Caswell and S. Tuljapurkar, eds), pp. 119–204. New York: Chapman & Hall.

de Roos, A.M., Diekmann, O. and Metz, J.A.J. 1992. Studying the dynamics of structured population models: a versatile technique and its application to *Daphnia. Am. Nat.*, **139**: 123–147.

de Roos, A.M., Metz, J.A.J., Evers, E. and Leipoldt, A. 1990. A size dependent predator–prey interaction: who pursues whom? *J. Math. Biol.*, **28**: 609–643.

Dieckmann, U. 1997. Can adaptive dynamics invade? *Trends Ecol. Evol.*, **12**: 128–131.

Dieckmann, U. and Doebeli, M. 1999. On the origin of species by sympatric speciation. *Nature*, **400**: 354–357.

Dieckmann, U. and Law, R. 1996. The dynamical theory of coevolution: a derivation from stochastic ecological processes. *J. Math. Biol.*, **34**: 579–612.

Diekmann, O., Mylius, S.D. and ten Donkelaar, J.R. 1999. Saumon à la Kaitala et Getz, sauce hollandaise. *Evol. Ecol. Res.*, **1**: 261–275.

Doebeli, M. and Dieckmann, U. 2000. Evolutionary branching and sympatric speciation caused by different types of ecological interactions. *Am. Nat.*, **156**: S77–S101.

Egas, M. 2002. Foraging behaviour and the evolution of specialisation in herbivorous arthropods. Doctoral dissertation, University of Amsterdam.

Eshel, I. 1983. Evolutionary and continuous stability. *J. Theor. Biol.*, **103**: 99–111.

Geritz, S.A.H. and Kisdi, É. 2000. Adaptive dynamics in diploid, sexual populations and the evolution of reproductive isolation. *Proc. R. Soc. Lond. B*, **267**: 1671–1678.

Geritz, S.A.H., Metz, J.A.J., Kisdi, É. and Meszéna, G. 1997. Dynamics of adaptation and evolutionary branching. *Phys. Rev. Lett.*, **78**: 2024–2027.

Geritz, S.A.H., Kisdi, É., Meszéna, G. and Metz, J.A.J. 1998. Evolutionarily singular strategies and the adaptive growth and branching of the evolutionary tree. *Evol. Ecol.*, **12**: 35–57.

Gurney, W.S.C. and Nisbet, R.M. 1985. Fluctuation periodicity, generation separation, and the expression of larval competition. *Theor. Pop. Biol.*, **28**: 150–180.

Heino, M., Metz, J.A.J. and Kaitala, V. 1997. Evolution of mixed maturation strategies in semelparous life histories: the crucial role of dimensionality of feedback environment. *Phil. Trans. R. Soc. Lond. B*, **352**: 1647–1655.

Hjelm, J., Persson, L. and Christensen, B. 2000. Growth, morphological variation and ontogenetic niche shifts in perch (*Perca fluviatilis*) in relation to resource availability. *Oecologia*, **122**: 190–199.

Jonsson, B. and Jonsson, N. 2001. Polymorphism and speciation in arctic charr. *J. Fish Biol.*, **58**: 605–638.

Kooijman, S.A.L.M. and Metz, J.A.J. 1984. On the dynamics of chemically stressed populations: the deduction of population consequences from effects on individuals. *Ecotoxicol. Environ. Safety*, **8**: 254–274.

Leonardsson, K. 1991. Predicting risk-taking behavior from life-history theory using static optimization techniques. *Oikos*, **60**: 149–154.

Lundvall, D., Svanbäck, R., Persson, L. and Byström, P. 1999. Size-dependent predation in piscivores: interactions between predator foraging and prey avoidance abilities. *Can. J. Fish. Aquat. Sci.*, **56**: 1285–1292.

Meszéna, G. and Metz, J.A.J. 1999. Species diversity and population regulation: the importance of environmental feedback dimensionality. Interim Report IR-99-045, IIASA, Laxenburg, Austria.

Metz, J.A.J. and Diekmann, O., eds. 1986. *The Dynamics of Physiologically Structured Populations*. Lecture Notes in Biomathematics Vol. 68. Berlin: Springer.

Metz, J.A.J., Nisbet, R.M. and Geritz, S.A.H. 1992. How should we define 'fitness' for general ecological scenarios? *Trends Ecol. Evol.*, **7**: 198–202.

Metz, J.A.J., Geritz, S.A.H., Meszéna, G., Jacobs, F.J.A. and van Heerwaarden, J.S. 1996a. Adaptive dynamics: a geometrical study of the consequences of nearly faithful reproduction. In *Stochastic and Spatial Structures of Dynamical Systems* (S.J. van Strien and S.M. Verduyn Lunel, eds), pp. 183–231. Amsterdam: North-Holland.

Metz, J.A.J., Mylius, S.D. and Diekmann, O. 1996b. When does evolution optimize? On the relationship between types of density dependence and evolutionarily stable life history parameters. Working Paper WP-96-04, IIASA, Laxenburg, Austria.

Meyer, A. 1990. Ecological and evolutionary consequences of the trophic polymorphism in *Cichlasoma citrinellum* (Pisces, Cichlidae). *Biol. J. Linn. Soc.*, **39**: 289–299.

Mittelbach, G.G. 1981. Foraging efficiency and body size: a study of optimal diet and habitat use by bluegills. *Ecology*, **62**: 1370–1386.

Mylius, S.D. and Diekmann, O. 1995. On evolutionarily stable life histories, optimization and the need to be specific about density dependence. *Oikos*, **74**: 218–224.

Persson, L. 1987. The effects of resource availability and distribution on size class interactions in perch, *Perca fluviatilis*. *Oikos*, **48**: 148–160.

Persson, L. and Greenberg, L.A. 1990. Optimal foraging and habitat shift in perch, *Perca fluviatilis*, in a resource gradient. *Ecology*, **71**: 1699–1713.

Persson, L., Leonardsson, K., de Roos, A.M., Gyllenberg, M. and Christensen, B. 1998. Ontogenetic scaling of foraging rates and the dynamics of a size-structured consumer–resource model. *Theor. Pop. Biol.*, **54**: 270–293.

Robinson, B.W. and Wilson, D.S. 1994. Character release and displacement in fishes: a neglected literature. *Am. Nat.*, **144**: 596–627.

Rundle, H.D., Nagel, J., Boughman, J.W. and Schluter, D. 2000. Natural selection and parallel speciation in sympatric sticklebacks. *Science*, **287**: 306–308.

Schliewen, U., Tautz, D. and Paabo, S. 1994. Monophyly of crater lake cichlids suggests sympatric speciation. *Nature*, **386**: 629–632.

Schluter, D. 1995. Adaptive radiation in sticklebacks: trade-offs in feeding performance and growth. *Ecology*, **76**: 82–90.

Schluter, D. 1996. Ecological speciation in postglacial fishes. *Phil. Trans. R. Soc. Lond. B*, **351**: 807–814.

Smith, T.B. and Skúlason, S. 1996. Evolutionary significance of resource polymorphisms in fishes, amphibians, and birds. *Annu. Rev. Ecol. Syst.*, **27**: 111–133.

Snorrason, S.S., Skúlason, S., Jonsson, B., Malmquist, H.J., Jonasson, P.M., Sandlund, O.T. and Lindem, T. 1994. Trophic specialization in arctic charr *Salvelinus alpinus* (Pisces, Salmonidae): morphological divergence and ontogenetic niche shifts. *Biol. J. Linn. Soc.*, **52**: 1–18.

Sogard, S.M. 1997. Size-selective mortality in the juvenile stage of teleost fishes: a review. *Bull. Mar. Sci.*, **60**: 1129–1157.

van Tienderen, P.H. and de Jong, G. 1986. Sex ratio under the haystack model: polymorphism may occur. *J. Theor. Biol.*, **122**: 69–81.

von Bertalanffy, L. 1957. Quantitative laws in metabolism and growth. *Quart. Rev. Biol.*, **32**: 217–231.

Wahlström, E., Persson, L., Diehl, S. and Byström, P. 2000. Size-dependent foraging efficiency, cannibalism and zooplankton community structure. *Oecologia*, **123**: 138–148.

Werner, E.E. 1988. Size, scaling, and the evolution of complex life cycles. In *Size-Structured Populations: Ecology and Evolution* (B. Ebenman and L. Persson, eds), pp. 60–81. Berlin: Springer.

Werner, E.E. and Gilliam, J.F. 1984. The ontogenetic niche and species interactions in size-structured populations. *Annu. Rev. Ecol. Syst.*, **15**: 393–425.

Werner, E.E. and Hall, D.J. 1988. Ontogenetic habitat shifts in bluegill: the foraging rate–predation risk trade-off. *Ecology*, **69**: 1352–1366.

Wilson, A.B., Noack-Kunnmann, K. and Meyer, A. 2000. Incipient speciation in sympatric Nicaraguan crater lake cichlid fishes: sexual selection versus ecological diversification. *Proc. R. Soc. Lond. B*, **267**: 2133–2141.

Wilson, D.S. and Yoshimura, J. 1994. On the coexistence of specialists and generalists. *Am. Nat.*, **144**: 692–707.

Ylikarjula, J., Heino, M. and Dieckmann, U. 1999. Ecology and adaptation of stunted growth in fish. *Evol. Ecol.*, **13**: 433–453.